POLARIZED CATHODOLUMINESCENCE STUDY OF $(InP)_2/(GaP)_2$ BILAYER SUPERLATTICE STRUCTURES

Y. TANG,* K. RAMMOHAN,* H.T. LIN,* D.H. RICH,* P. COLTER** and S.M. VERNON**
*Department of Materials Science and Engineering, University of Southern California, Los Angeles, CA 90089-0241
**Spire Corporation, Bedford, MA 01730

ABSTRACT

Linearly polarized cathodoluminescence (LPCL) imaging and spectroscopy techniques have been employed to examine the optical properties and homogeneity of $(InP)_2/(GaP)_2$ bilayer superlattice (BSL) structures which exhibit a lateral composition modulation that leads to the formation of quantum wires. LPCL spectra were measured for various temperature and electron beam excitation densities. The magnitude of the polarization anisotropy and spectral lineshape are found to depend sensitively on the excitation conditions, revealing large nonlinear optical effects in these samples. CL images reveal that defects in the bilayer superlattice structure originate from the GaAs substrate or the initial stages of InGaP growth.

INTRODUCTION

Nonlinear optical properties of III-V semiconductors have attracted a great deal of interest since they are important for applications in optical communication such as switching, amplification and signal processing. An important nonlinear optical property is the change in excitonic absorption (in energy, polarization, and intensity) that results from phase-space filling of carriers in one- and two-dimensionally confined systems, i.e., quantum wells and wires.[1,2] This property is analogous to the Burstein-Moss band filling which occurs in bulk semiconductors and raises the energy of the unoccupied electron and hole states as the excitation intensity increases. As the dimensionality of the confined system increases from 1-D to 2-D, the narrowing of the density of states will exhibit a lower excitation threshold for phase-space filling, thereby yielding potentially enhanced nonlinear optical effects. In this study, we have examined $(InP)_2/(GaP)_2$ bilayer superlattices which exhibit a lateral composition modulation that leads to the formation of quantum wires. Previous reports have shown that a spontaneous composition modulation along the [110] direction occurs and is induced by strain.[3-7] Optical measurements have found evidence supporting the existence of quantum wires due to the quantum confinement along both the growth direction and the composition modulation direction.[4,6,7] In this paper, linearly-polarized cathodoluminescence (LPCL) spectroscopy and imaging techniques have been employed to examine the polarization anisotropy and excitation dependence of the luminescence from $(InP)_2/(GaP)_2$ bilayer superlattice (BSL) structures. We observe new nonlinear optical effects in this structure, as evidenced by large variations in the BSL excitonic transition energy and polarization anisotropy as the excitation density is varied.

EXPERIMENTAL

The bilayer superlattice was grown using metal-organic chemical vapor deposition with the GaAs substrates maintained at T = 650° C. Initially, 3000 Å of lattice-matched $In_{0.49}Ga_{0.51}P$ was grown on a GaAs(001) substrate misorientated 3° towards (111)A. Each $(InP)_2$ and $(GaP)_2$ bilayer was grown in a time interval of ~10 sec, after which the system was purged to prepare

Mat. Res. Soc. Symp. Proc. Vol. 379 © 1995 Materials Research Society

for the succeeding bilayer. A total of 20 periods of $(InP)_2/(GaP)_2$ were grown giving a thickness of ~200 Å. Finally, a 3000 Å $In_{0.49}Ga_{0.51}P$ capping layer was grown. All three samples (labeled 2979, 2980, 2983) were grown with nominally the same growth conditions. As evidenced by the data to be presented below, slight variations in growth condition, e.g., as in growth rates and sample temperature occurred, yielding differences in the optical quality between the three samples. Transmission electron microscopy (not shown here) revealed that the periodicity of the lateral ordering ranged from ~800 to ~1000 Å.

The LPCL experiments were performed with a modified JEOL-840A scanning electron microscope using a 10 keV electron beam with probe currents (I_b) ranging from 50 pA to 30 nA. The samples were maintained at a temperature of ~87 K and the luminescence signal was dispersed by a 0.25 m monochromator and detected by a cooled GaAs:Cs photomultiplier tube (PMT). The spectral resolution was ~2 nm. Polarization measurements were performed by rotating a polarizer *in vacuo* so as to detect luminescence with the electric field, E, along [110] and [1$\bar{1}$0] directions.[8]

RESULTS AND DISCUSSION

Spatially-integrated non-polarized and linearly polarized CL spectra (T=87 K) for the three samples are shown in Fig. 1. Non-polarized spectra were normalized to the same peak intensity. Each pair of polarized spectra was normalized with the same factor and offset below the non-polarized one. Two kinds of emissions were observed in the wavelength range from 600 to 800 nm. First, luminescence at the shortest wavelengths shown corresponds to the emission from the InGaP bulk (i.e. the buffer and capping layers). Second, another luminescence feature with lower energy is found to originate from the BSL layers. In sample 2979, only one peak was observed at an energy of ~110 meV lower than the InGaP emission. However, two additional broad

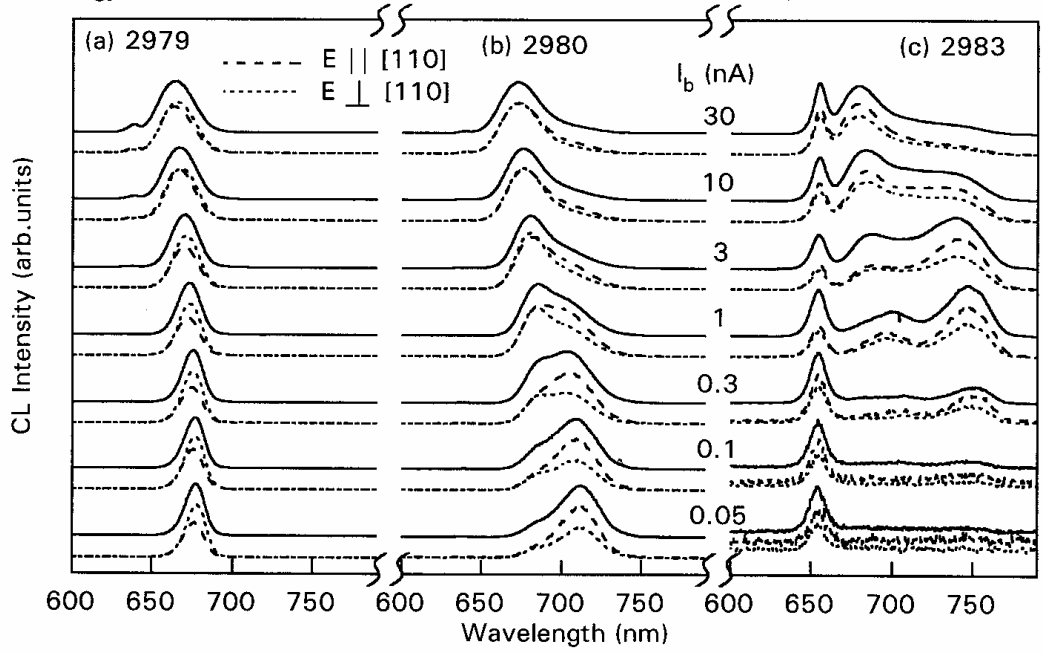

Fig. 1 Stack plots of spatially-integrated non-polarized (solid line) and linearly polarized (dashed lines) CL spectra taken for various probe currents in sample 2979 (a), 2980 (b) and 2983 (c).

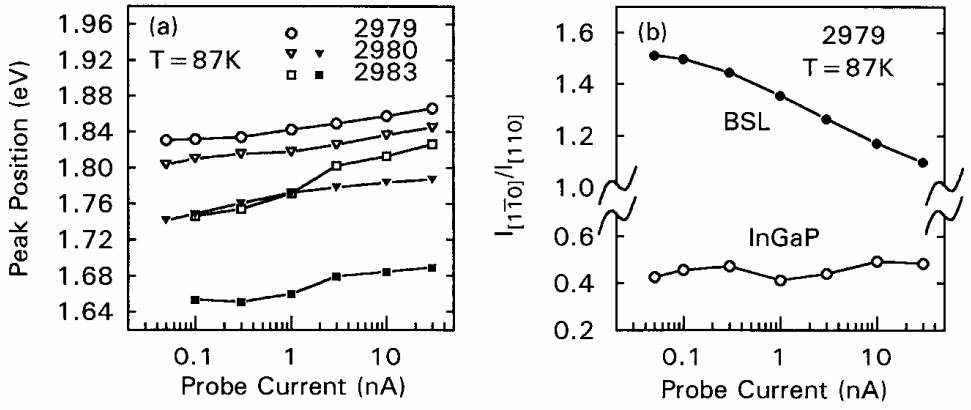

Fig. 2 Plots of peak positions (a) and polarization ratio (b) as a function of probe current.

luminescence peaks are observed in the wavelength range from 650 to ~750 nm in samples 2980 and 2983.

From Fig. 1, it is apparent that the energy of the InGaP bulk luminescence remains constant for different beam currents but varied for different samples. This probably indicates a small variation of the $In_xGa_{1-x}P$ alloy composition x for the different samples. The lowering of transition energy for emission from the BSL is due to the lateral composition modulation, as previously reported.[3-7] The lateral ordering along [110] results in In- and Ga-rich regions, in which there is a concomitant lateral band gap variation. Previous band-energy calculations for a similar BSL structure by Mascarenhas *et al.*,[7] who assumed a coherency strain condition, showed that heavy- and light-holes (hh and lh) are confined in the In- and Ga-rich regions, respectively, resulting in type-I and type-II lateral superlattices for heavy- and light-holes, i.e. e-lh transitions, while lower in energy by ~48 meV compared to that for e-hh transitions, are spatially indirect transitions.[7] The relative contribution of the e-hh and e-lh transitions is expected to involve an interplay between the electron-hole wavefunction overlap and occupation density. At low excitation densities, when the hh states are negligibly populated, the lh-states will dominate in the luminescence lineshape. At higher excitation conditions (higher beam currents or higher temperatures), the quasi-Fermi level for holes will move closer to the hh-levels, resulting in an enhanced occupation density of heavy-holes, thereby enhancing the e-hh contributions in the spectra. In order to test this hypothesis, we have examined the CL lineshapes for various temperatures and excitation currents. The peak energy position, at which there is a maximum in CL intensity, shifted from 1.830 eV under a probe current of 50 pA to 1.866eV under current of 30 nA in sample 2979. Fig. 2(a) shows the plot of peak position as a function of probe current for sample 2979. Such nonlinear optical behavior is consistent with the band-filling effects discussed. Likewise, for the other two samples, there is an increase in the energy of the peaks as the beam current increases. The positions of two BSL peaks found for 2980 and 2983 are plotted in Fig. 2(a). The presence of two peaks may indicate an increase in disorder relative to sample 2979 where only one peak was resolved (see CL imaging below).

The polarization ratio, $I_{[1\bar{1}0]}/I_{[110]}$, which is defined as the ratio of CL intensities detected with the electric field **E** of the polarizer oriented parallel to $[1\bar{1}0]$ and [110], respectively, is about ~0.5 for InGaP emission in all three samples. This is consistent with the model that predicts a CuPt-like ordering structure in $In_xGa_{1-x}P$ material.[9,10] Figure 2(b) shows the polarization ratio as a function of probe current. The BSL luminescence is polarized along the $[1\bar{1}0]$ direction in sample 2979; the polarization ratio $I_{[1\bar{1}0]}/I_{[110]}$ varies from ~1.5 to 1.1 as I_b increases from 50 pA

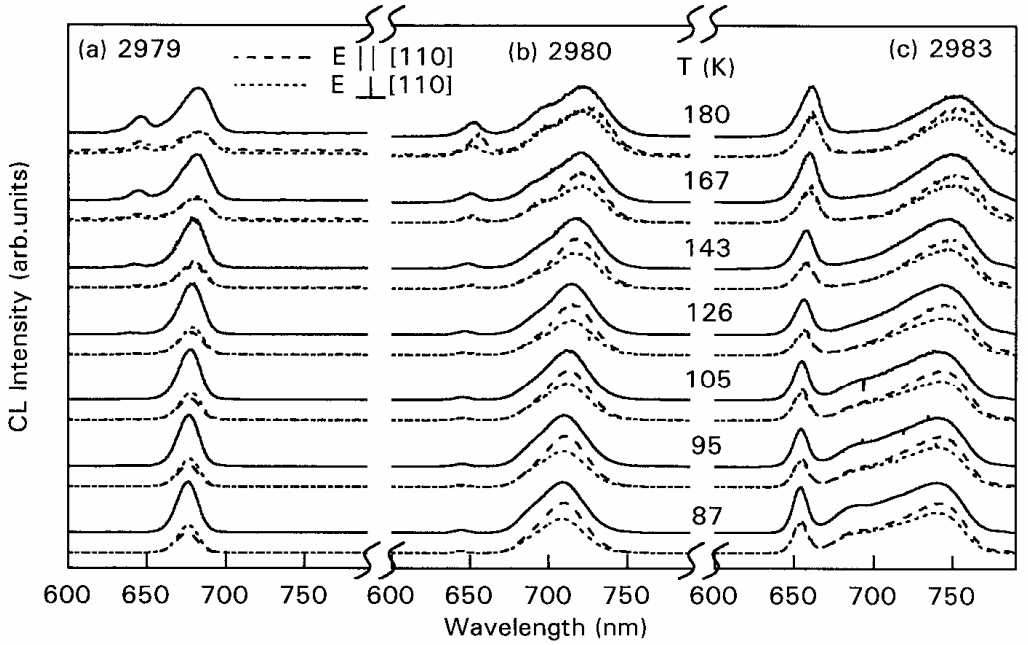

Fig. 3 Stack plots of spatially-integrated non-polarized (solid line) and linearly polarized (dashed lines) CL spectra taken at temperature ranging from 87 to 180 K for sample 2979 (a), 2980 (b) and 2983 (c).

to 30 nA. This nonlinear polarization effect can also be explained by band-filling effects. The e-hh and e-lh transitions, in strained and quantum confined-systems will generally exhibit an orthogonal polarization dependence.[8,11,12] By altering the relative contributions of the e-hh and e-lh transitions in the spectra by changing I_b, a variation in the polarization ratio is observed.

The temperature dependence of CL emissions for these three samples was examined. Figure 3 shows a stack plot of LPCL spectra for temperatures varying from 87 to 180 K. Probe currents of 0.3, 1, and 3 nA were used for samples 2979, 2980 and 2983, respectively. In sample 2979, the polarization ratio $I_{[1\bar{1}0]}/I_{[110]}$ for BSL emission decreases with increasing temperature, but remains almost constant for InGaP bulk emission. Figure 4 shows a plot of polarization ratio as a function of temperature. The relative intensity of the BSL emission with respect to the InGaP bulk emission reduces as the temperature increases. The decrease of polarization ratio with increasing temperature for sample 2979 is also consistent with a variation of the e-hh and e-lh contributions to the luminescence resulting from the thermal redistribution of holes according to Fermi-Dirac statistics as the temperature is increased. For very low temperatures, almost all holes are confined to the lowest energy state (lh-potential). As the temperature increases, thermal redistribution of holes into the hh states will occur, and again result in an enhancement of the e-hh contribution, thereby changing the polarization ratio as shown in Fig. 4. A much smaller polarization variation as a function of temperature is observed in Fig. 4 for samples 2980 and 2983. The enhanced defect density in

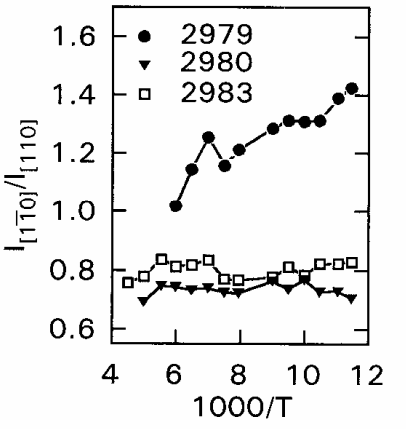

Fig. 4 Plot of polarization ratio $I_{[1\bar{1}0]}/I_{[110]}$ as a function of temperature.

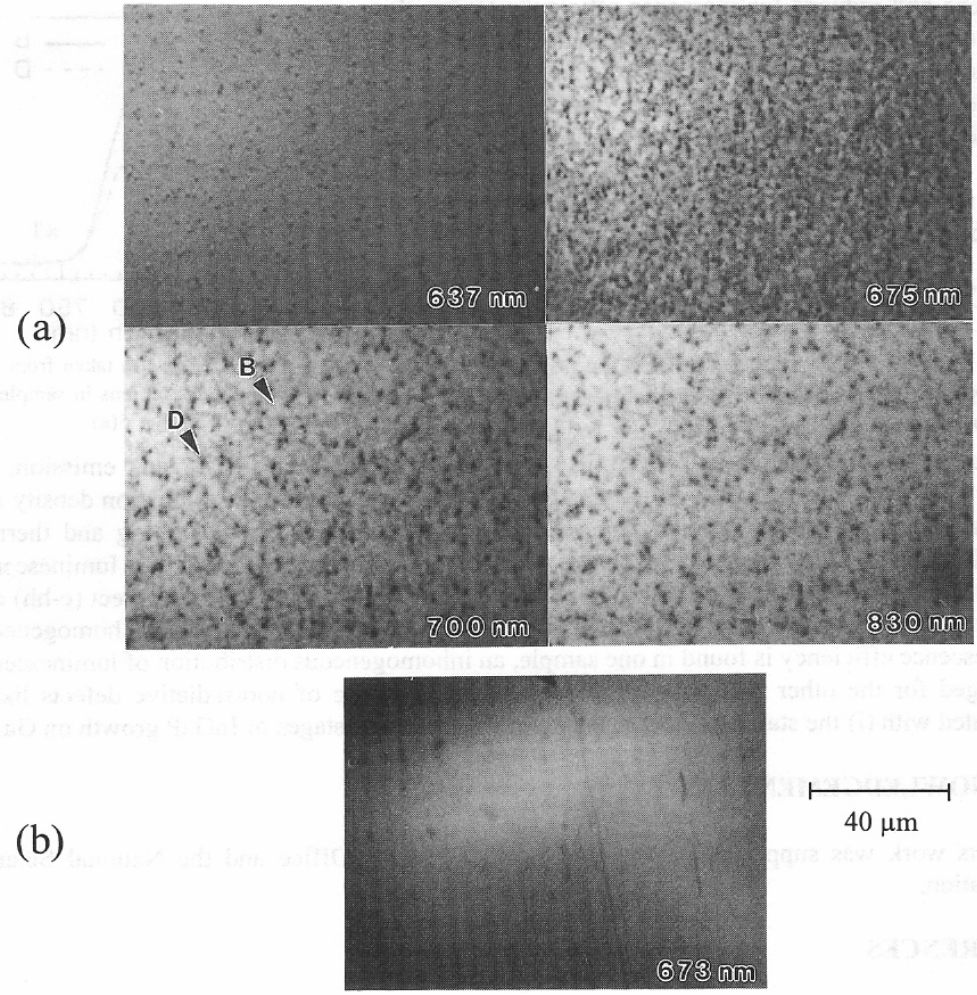

Fig. 5 Monochromatic CL images in (a) sample 2980 with λ = 637, 675, 700, 830 nm, respectively, and (b) sample 2979 with λ = 673 nm.

these samples (see CL images) apparently influences the thermal redistribution of e-hh and e-lh transitions, owing to an additional large presence of competing nonradiative channels. Moreover, a local strain relaxation in close proximity to these defects will reduce the magnitude of the hh-lh band splitting, thereby also reducing the redistribution of holes as the temperature is changed.

Monochromatic CL imaging was used to examine the spatial homogeneity of the samples and is shown in Fig. 5. The CL images for 2979 indicate a high-degree of homogeneity (on a scale of ~μm) as observed for monochromatic images corresponding to emissions from the GaAs substrate, BSL layer and InGaP bulk layers. A substantial inhomogeneity, however, appears in samples 2980 and 2983, as shown in Fig. 5(a) for 2980, indicating a presence of growth-related non-radiative defects. The images for 2983 (not shown) are very similar. In sample 2980, the spatial correlation among CL images taken over the same region with emission wavelengths corresponding to the GaAs substrate (830 nm), InGaP buffer (637 nm) and bilayer superlattice (675 and 700nm) shows that non-radiative defects arise most likely from defects formed during the initial stages of growth on the GaAs substrate. Local CL spectra taken from regions with

enhanced and reduced luminescence efficiency in sample 2980 (Fig. 6) shows that longer wavelength emission dominates at regions with reduced luminescence while at regions with enhanced luminescence shorter wavelength emission dominates. These nonradiative defects are related to the growth conditions and SEM topography shows a rough surface on sample 2983, which is likely the result of three dimensional growth.

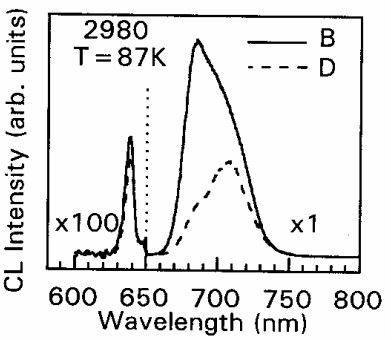

Fig. 6 Local CL spectra taken from the bright and dark regions in sample 2980 as marked in Fig. 5(a).

CONCLUSION

In conclusion, we have examined the nonlinear optical properties in $(InP)_2/(GaP)_2$ bilayer superlattice structures. A CuPt-like structural ordering in the InGaP bulk results in an observed polarization anisotropy in luminescence. Unlike the InGaP bulk emission, the energy and polarization of BSL emission strongly depend on the external excitation density and thermal excitation. Such nonlinear optical behavior is attributed to band-filling and thermal redistribution of holes confined to heavy- and light-hole states. The resulting luminescence intensity and polarization ratios will involve an interplay between the spatially direct (e-hh) and indirect (e-lh) electron-hole overlap integrals, and occupation probability. While a homogeneous luminescence efficiency is found in one sample, an inhomogeneous distribution of luminescence is imaged for the other two samples, indicating the presence of non-radiative defects likely associated with (i) the starting GaAs substrate or (ii) the initial stages of InGaP growth on GaAs.

ACKNOWLEDGEMENT

This work was supported by the U.S. Army Research Office and the National Science Foundation.

REFERENCES

1. S. Schmitt-Rink, D. S. Chemla, D. A. B. Miller, Adv. Phys, **38**, 89 (1989).
2. V. D. Kulakovskii, E. Lach, and A. Forchel, Phys. Rev. B **40**, 8087 (1989).
3. K. C. Hsieh, J. N. Baillargeon and K. Y. Cheng, Appl. Phys. Lett. **57**, 2244 (1990).
4. P. J. Pearah, E. M. Stellini, A. C. Chen, A. M. Moy, K. C. Hsieh and K. Y. Cheng, Appl. Phys. Lett. **62**, 729 (1993).
5. K. Y. Cheng, K. C. Hsieh and J. N. Baillargeon, Appl. Phys. Lett. **60**, 2892 (1992).
6. A. C. Chen, A. M. Moy, P. J. Pearah, K. C. Hsieh and K. Y. Cheng, Appl. Phys. Lett. **62**, 1359 (1993).
7. A. Mascarenhas, R. G. Alonso, G. S. Horner, S. Frœyen, K. C. Hsieh and K. Y. Cheng, Photovoltaic Advanced Research and Development Project, edited by Rommel Noufi (AIP Conference Proceedings 268, Denver, CO, 1992) pp. 125-130.
8. Y. Tang, D. H. Rich, E. H. Lingunis, and N. M. Haegel, J. Appl. Phys. **76**, 3032 (1994).
9. A. Mascarenhas, S. Kurtz, A. Kibbler and J. M. Olson, Phys. Rev. Lett. **63**, 2108 (1989).
10. Y. Ueno, Appl. Phys. Lett. **62**, 553 (1993).
11. J. S. Weiner, D. S. Chemla, D. A. B. Miller, H. A. Haus, A. C. Gossard, W. Wiegmann, C. A. Burrus, Appl. Phys. Lett. **47**, 664 (1985).
12. P. C. Sercel and K. J. Vahala, Phys. Rev. B **44**, 568 (1991).